Contract No.:

This manuscript has been authored by Savannah River Nuclear Solutions (SRNS), LLC under Contract No. DE-AC09-08SR22470 with the U.S. Department of Energy (DOE) Office of Environmental Management (EM).

Deep and shallow traps analysis in semi-insulating CdZnTe

Kihyun Kim*

Department of Radiologic Science, Korea University, Seoul 02841, Republic of Korea

School of Health and Environmental Science,

Korea University, Seoul 02841, Republic of Korea

Yongsu Yoon

Department of Health Sciences, Graduate School of Medical Sciences,

Kyushu University, Fukuoka 812-8582, Japan.

Ralph B. James

Sivannah River National Laboratory, Aiken, SC 29808 USA.

(Dated: November 27, 2017)

Abstract

Trap levels which are deep or shallow play an important role in electrical and optical properties of semiconductor thereby trap level analysis is very important in most of semiconductor devices. Deep-level defects in CdZnTe are essential in Fermi level pinning at the middle of bandgap and also be responsible for incomplete charge collection and polarization effects. However, deep level analysis in semi-insulating CdZnTe (CZT)is very difficult. Theoretical capacitance calculation of metal/insulator/CZT (MIS) device with deep-level defects exhibit inflection points when the donor/accoptor level crosses the Fermi level in the surface-charge layer (SCL). Three CZT samples with the different resistivities, that is, 2×10^4 (n-type), 2×10^6 (p-type), and 2×10^{10} (p-type) Ω·cm, were used in fabricating MIS CZT devices. These devices showed several peaks in their capacitance measurements due to upward/downward band bending, which depends on the surface potential. Theoretical and experimental capacitance measurements are well agree except in fully compensated case.

PACS numbers: 71.55.-i, 73.40,Qv, 71.55.Gs, 85.30.De

Keywords: CdZnTe, trap level, MIS devices, Capacitance measurement

* khkim1@korea.ac.kr

I. INTRODUCTION

CdTe and CdZnTe (CZT) are the best semiconductor materials to detect X- or γ-rays at room temperature. It is well known that a deep trap level pins the Fermi level in the middle of bandgap and it is indispensable feature in semi-insulating materials. However, several authors argued that such deep traps are responsible for polarization, which deteriorate detector performance of incomplete charge collection [1, 2]. Identification of deep level traps by electro-optical methods, such as current deep-level transient spectroscopy (I-DLTS)[3] and thermoelectric emission spectroscopy(TEES) [4] is limited by thermal noise. Furthermore, optical methods, such as photoluminescence (PL) and photo-ionization are limited in detecting deep levels due to low radiative recombination rates and thermal noise, respectively.

Generally, the analysis of the capacitance-voltage (C-V) behaviour of a metal-insulator-semiconductor (MIS) device is a convenient method to delineate the electrical properties of the interface between the semiconductor and the dielectric layer [5]. However, if deep bulk levels exist, C-V data are strongly affected by small bias changes, as shown in Fig. 1. Assuming all basic features of semiconductors, including deep bulk levels, we developed a theoretical model of a MIS structure based on CZT. Our analysis can improve our understanding of deep-level defects in CZT and their concentrations, as well as our understanding of the characteristics of MIS devices.

II. EXPERIMENTS

A. Sample preparation

All CZT crystals used in this experiment were grown by the traveling heater method (THM) at 850°C. Indium-doped polycrystalline CZT were used as a feeding material. Usually, the doped indium melt down in Te solvent zone so few ppm level was doped in feed CZT material. The growth rate was 3.5 mm/day and cooling rate was adjusted 0.5 $^{\circ}\mathrm{C}$/min. As grown 1-inch diameter CZT ingots are sliced parallel to the growth direction and selected single crystal region. CZT samples were prepared by chemical and mechanical polishing with alumina powder and Br-MeOh solutions. The samples were dipped in 0.05% Br-MeOH for 600 s to remove their stressed surface layers, and to ensure ohmic contact after mechanical- and chemical-polishing. Electro-less Au contacts were applied to one or two side of the CZT samples with $AuCl_3$ (5%) depending on the MIS device fabrication or electrical characterization, respectively. The electrical resistivities of

the three CZT samples obtained from three CZT ingots were 1×10^6, 2×10^{10}, and 1×10^4 Ω·cm doped with 5×10^{14}, 5×10^{15}, and 5×10^{16} cm^{-3} of indium, respectively. Insulating layer was formed directly on the surfaces of the semiconductor using a solution of $NH_4F/H_2O_2/H_2O$ (2.86 g/ 8 ml/ 17 ml) which are generally used in the formation of passivation layer [6]. The thickness of insulating layer was about 2 μm for all samples. The MIS devices were completed by depositing, via an e-beam, multiple Au contacts of 1×1 mm^2 on the insulating layer. Finally, CZT samples were mounted on printed circuit board (PCB)for the C-V measurement, as shown in Fig. 2.

B. Trapping and detrapping time

The trapping τ_t and detrapping time τ_{dt} of donors which ionized positively given by

$$\tau_{\mathrm{t}} = \frac{1}{v_{th} N_t \sigma}, \tag{1}$$

$$\tau_{\mathrm{dt}} = \frac{1}{N_C \sigma v_{th}} \exp\left(\frac{E_C - E_t}{kT}\right), \tag{2}$$

where N_C is the effective density of states for the conduction band, σ is the donor capture cross section, v_{th} is the thermal velocity of electron,N_t is the trap concentrations of the donor level, E_t is the energy of the donor level, and E_C is the energy of the conduction band. The detrapping time depends on the capture cross section and the trap level of the donor whereas the trapping time depends on the capture cross section and the trap concentrations of donor. For example, the detrapping time at E_t = 0.5 eV with the capture cross section of 1×10^{-13} cm^2 is 1×10^{-4} s at 300 K, respectively. The trapping and detrapping time for the electrons is shown in Fig. 3 as a function of the trap level for CZT at room temperature, assuming an average trap cross section of 10^{-13} cm^2 and the trap concentrations of 10^{12} cm^{-3} [3, 7]. The procedure for taking C-V measurements involves the application of DC bias voltages across the capacitor while making the measurements with an AC signal. Commonly, AC frequencies from about 10 kHz to 10 MHz are used for these measurements. Several AC frequency considering the trap levels were chosen for the C-V measurement [8].

III. THEORETICAL BACKGROUND

We simulated at 300K the C-V measurements of CZT (Zn=10%) with the six traps that are commonly observed in CdTe compounds via DLTS measurement [5]. Table 1 thoroughly summa-

rizes the assumed traps and trap levels for the C-V calculations. The concentrations of the traps were adjusted to their proper values depending on the sample's resistivity, that is, the Fermi level, using a compensation mechanism. The height of the potential barrier of the interface between the metal and the CZT was set to 0 V. Also, the band-gap of the CZT was calculated with following equation:

$$\mathrm{E_g(x,T) = E_0 + a_1 x + a_2 x^2 - \frac{a_3 T^2}{a_4 + T} \quad (eV)}, \tag{3}$$

where, $\mathrm{E_0}$ = 1.606 eV, $\mathrm{a_1}$ = 0.38 eV, $\mathrm{a_2}$ = 0.463 eV, $\mathrm{a_3}$ = 4.5 $\times$ 10^{-3} eV/K, and $\mathrm{a_4}$ = 264 K.

Using the charge neutrality condition, the Fermi level position were calculated by setting the surface potential to 0 V via the following:

$$\mathrm{p + N_{SD}^{+} + N_{DD1}^{+} + N_{DD2}^{+} = n + N_{SA}^{-} + N_{DA}^{-} + N_{AC}^{-}}. \tag{4}$$

The total charge $\mathrm{Q}_{sc}(\psi)$ and total capacitance $\mathrm{C}_{sc}(\psi)$ in the surface-charge layer (SCL) were calculated by solving the one-dimensional Poisson equation on the surface potential,

$$\mathrm{\frac{d^2\psi(x)}{dx^2} = -\frac{q}{\epsilon_s}\rho_c(x)}, \tag{5}$$

where $\psi(x)$ is the band bending potential, ϵ_s is the permittivity of CZT, ρ_c(x) is the charge density in the semiconductor, and q is the electron's charge.

The formula related to the charge density can be written as

$$\mathrm{\rho_c(x) = p(x) + N_{SD}^{+}(x) + N_{DD1}^{+}(x) + N_{DD2}^{+}(x) - n(x) - N_{SA}^{-}(x) - N_{AC}^{-}(x) - N_{DA}^{-}(x)}. \tag{6}$$

In solving Eq. 5, both sides were multiplied by $2\frac{d\psi}{dx}$, and Eq. 6 was substituted into Eq. 5, yielding

$$\mathrm{2\frac{d\psi}{dx}\frac{d^2\psi}{dx^2} = -2\frac{q}{\epsilon_s}\rho_c(x)\frac{d\psi_s}{dx}}. \tag{7}$$

Using integration by substitution from the surface to the bulk, the equation could be solved about the electric field with the surface potential

$$\begin{aligned} \left(\frac{d\psi_s}{dx}\right)^2 &= -2\frac{q}{\epsilon_s}\int_0^{\psi_s}\rho_c(x)d\psi \\ \frac{d\psi_s}{dx} &= \sqrt{-2\frac{q}{\epsilon_s}\int_0^{\psi_s}\rho_c(x)d\psi}. \end{aligned} \tag{8}$$

In the MIS structure, the total charge in the SCL could be calculated with the equation

$$\mathrm{Q_{sc} = \epsilon_s E}, \tag{9}$$

where the electric field was $\mathrm{E} = -\dfrac{\mathrm{d}\psi_\mathrm{s}}{\mathrm{dx}}$. Also, the total capacitance in the SCL was derived from the equation

$$\mathrm{C_{sc}} = -\frac{\mathrm{dQ_{sc}}}{\mathrm{d}\psi_\mathrm{s}}, \tag{10}$$

and its resistivity was calculated with the equation

$$\rho = \frac{1}{\mathrm{qp}\mu_\mathrm{h} + \mathrm{qn}\mu_\mathrm{e}}, \tag{11}$$

where p is the hole's density, n is the electron's density, μ_h is the hole's mobility (μ_h = 100 $\mathrm{cm^2/V{\cdot}s}$), and μ_e is the electron's mobility (μ_e = 1100 $\mathrm{cm^2/V{\cdot}s}$). The Fermi energy was shifted, and the band was flexed relatively when it was bent according to the band-bending potential. All the parameters and statistics used in the theoretical calculations were thoroughly described in references [9] and [10].

IV. RESULTS AND DISCUSSION

A. Simulation

Fig. 4 shows the simulated charge and capacitance per unit area due to each trap for the semi-insulating case, that is, $\mathrm{E_F}$ = 0.778 eV. In this case, CZT had almost its intrinsic carrier concentration of $\sim 10^6$ $\mathrm{cm^{-3}}$ and its resistivity was 4.1×10^{10} $\Omega{\cdot}$cm. In the calculations, we set the Fermi level to a flat band-voltage to visualize the traps' relative positions more easily. The electrons and holes accumulated at the SCL for negative- and positive-surface potentials as shown in Fig. 4(a). Fig. 4(b) shows each trap's contribution to the space charge for positive- and negative-bias; shallow impurities symmetrically contributed to the space-charge for both biases. Also, deep acceptors and A-centers contributed nearly the same amounts and in the manner. However, both deep donors exhibited asymmetric patterns and their contribution were prominent for the negative surface's potential. Fig. 4(c) shows the total capacitance per area in the SCL for positive- and negative-bias. Two peaks appear, at $\mathrm{E_V}$ + 0.41 eV and $\mathrm{E_V}$ + 0.76 eV, which are the same as the trap levels of the deep donors. To confirm the origin of these peaks, we calculated each trap's contribution to the total capacitance, as shown in Fig. 4(d). We observed a clear curvature due to deep donors 1 and 2, as indicated by the dotted circle. Undoubtedly, the two peaks observed in the capacitance versus. surface potential originated from deep donors 1 and 2.

We simulated the effects of the deep donors' concentration on capacitance versus surface potential by retaining same Fermi energy while changing each trap's concentration and maintaining compensation. The traps with relatively low concentrations did not exhibit any peaks in the capacitance versus surface potential, whether they were located in deep- or shallow-levels.

The effects of deep-level defects on the capacitance were simulated for E_F = 0.525 eV by keeping all defect levels the same but using different concentrations of traps. In this case, the resistivity of CZT was 3.08 $\times$ 10^6 Ω·cm. As shown in Fig. 5(a), depletion and inversion occurred with a positive surface potential due to the downward bending of the band. In this case, the density of the majority carrier(holes) decreased whereas the minority carrier (electrons) density increased in just the SCL. For the negative potential, the density of the majority carrier density at the surface was higher that that in the bulk. Each trap contributed symmetrically to the total charge for both negative- and positive-bias, except for deep donor 2, as shown in Fig. 5(b). The total capacitances for the positive- and negative-surface potentials are shown in Fig. 5(c). We observe two clear peaks around 0.41 eV and 0.76 eV from the valence band that correspond to deep donor 1 and 2, respectively, and are clearly shown in Fig. 5(d). For the negative surface-potential, the band bent downward, and the ionization of deep donor 2 began when the Fermi level just crossed the level of deep donor 2. For the positive surface potential, the band bent upward. The fully ionized deep donor 1 begun to neutralize at the SCL when the Fermi level just crossed the level of deep donor 1. Both cases induced variations in the total SCL charge and total capacitance.

From the theoretical simulation, we determined that both of these changes in the SCL of a CZT MIS device are mainly affected by the traps' positions relative to the Fermi level and the traps' concentrations relative to their overall concentration.

B. Experiment

First, C-V measurements were acquired from the CZT sample with a resistivity of 1 $\times$ 10^4 Ω·cm. This CZT sample was doped with 5 $\times$ 10^{16} cm^{-3} of indium, and thus exhibited n-type properties in the Hall measurements. The work functions of gold [11] and CZT were 5.1 eV and 4.56 eV, respectively. The work function of CZT was estimated from the current-voltage curve as lying between 220 K and 300 K. The current density, J, was determined from the equation

$$J(T) = A^* T^2 \exp\left(-\frac{q\phi_b}{kT}\right), \tag{12}$$

where A^* is Richardson constant, and ϕ_b is barrier height. The work functions obtained from metal/CZT and metal/insulator/CZT may differ slightly, but here we used the work function obtained from the former. Also, the lowering of barrier height (0.1 eV) due to an imaging force was considered.

Fig. 6 shows C-V measurement above CZT sample corresponding to 100-kHz frequency. As the mobility of charge carriers is low, we could not identify any dependence on frequency. A pole at - 0.6 eV was observed in the capacitance measurements. The flat band voltage between n-type CZT and gold is - 0.44 eV, so the position of the actual trap is 0.16 eV. This level correspond to the A-center level, which is a complex of a Cd vacancy (V_{Cd}) and indium [7]. For this sample, the concentration of the indium dopant exceeded the compensation level so hence, A-center level was higher than that of Cd vacancies.

Fig. 7 shows second set of C-V measurements for the CZT sample with a resistivity of 2×10^6 Ω·cm. The work functions of gold and CZT were 5.1 eV and 5.55 eV, respectively. The flat band voltage was 0.55 eV, considering that the lowering of barrier-height due to an image force. The capacitance measurements showed one pole at 0.54 eV. The actual trap level considering the flat band voltage was 1.09 eV. This trap was not considered in the theoretical model and frequently appears in other papers [3, 4, 12, 13]. The origin of this defect is not clear, but it always appears, regardless of the stoichiometry, growth method, growth temperature, or conductivity. So it may be related to microstructural defects, such as dislocations [12], rather than to the positively-charged tellurium vacancy.

Finally, C-V measurements were conducted for the CZT sample with a resistivity of 2×10^{10} Ω·cm. The work functions of gold and CZT were, respectively, 5.1 eV and 5.21 eV. However, the CZT sample already was in the fully depleted state, so the capacitance did not change with the bias and the frequency.

The C-V analysis for the two low resistivity samples showed that traps located near the Fermi level exhibit peaks. In the theoretical calculations, the traps' positions relative to the Fermi level and their concentration relative to those of the other traps were the most important factors influencing the C-V measurements.

V. CONCLUSIONS

We successfully grew a high-resistivity CZT material by the THM. Depending on the In dopant's concentration, the CZT samples exhibited different degrees of compensation. Capacitance measurements for the MIS CZT device showed different shapes of capacitance curves. For the low-resistivity n-type CZT sample, a 0.16-eV peak was dominant. As-grown CZT samples contain Cd vacancies, but this CZT sample was doped with 5×10^{16} cm^{-3} of indium, so the A-center level concentrations were expected to be dominant. For a medium-doped sample, at the 1.09-eV level, dislocations induced defect was dominant. However, since the semi-insulating CZT sample was already fully compensated, it did not give any useful information on energy levels.

The existence of deep traps in semi-insulating CZT can be confirmed with fully uncompensated CZT samples which have resistivity of, for example, $5 \times 10^8 \sim 1 \times 10^9$ Ω·cm.

ACKNOWLEDGMENTS

This work was supported primarily by a grant (NRF-2015M2B2A9032788) of the National Research Foundation of Korea (NRF) funded by the Ministry of Science, ICT and Future Planning (MSIP), Republic of Korea.

[1] G. S. Camarda, A. E. Bolotnikov, *et al.*, IEEE Trans. Nucl. Sci. **55**(6) 3725 (2008).

[2] D. S. Bale, S. A. Soldner, and C. Szeles, Appl. Phys. Lett. **92**, 082101 (2008).

[3] R. Gul, K. Keeter, R. Rodriguez, *et al.*, J. Electron. Mater. **41**(3), 488 (2012).

[4] A. Castaldini, A. Cavallini, B. Fraboni, P. Fernandez and J. Piqueras, J. Appl. Phys. **83**, 2121 (1998).

[5] K. G. Germanova and E. P. Valcheva, Revue Phys. Appl. **22**, 985-989, (1987).

[6] K. H. Kim, R. Tappero, A. E. Bolotnikov, *et al*, J. Korean. Phys. Soc. **66** (10), 1532 (2015).

[7] R. Gul, A. Bolotnikov, K. H. Kim, *et al* , J. Electro. Mater. **40** (3). 274 (2011).

[8] I. Farella, G. Montagna, A. M. Mancini, and A. Cola, IEEE Trans. Nucl. Sci. **56** (4), 1736 (2009).

[9] E. Nicollian and J. Brews, *MOS(Metal Oxide Semiconductor) Physics and Technology* (Wiley, New York, 1982).

[10] J. Blakemore, *Semiconductor Statistics* (Dover, New York, 1987).

[11] H. B. Michaelson, J. Appl. Phys. **48**, 4729 (1977).

[12] K. H. Kim, J. H. Choi, A. E. Bolotnikov, *et al*, J. Korean Phys. Soc. **62**(4), 623 (2013).

[13] J. Zázvorka, J. Franc, V. Dědič, and M Hakl, JINST **9**, C04038 (2014).

TABLE I. Types of traps and trap levels used in the simulations of capacitance.

Trap	Trap level (eV)
Valence band	$E_V = 0$
Shallow acceptor	$E_{SA} = E_V + 0.009$
A-center	$E_{AC} = E_V + 0.16$
Deep acceptor	$E_{DA} = E_V + 0.34$
Deep donor 2	$E_{DD2} = E_V + 0.41$
Deep donor 1	$E_{DD1} = E_V + 0.76$
Shallow donor	$E_{SD} = E_C - 0.014$
Conduction band	$E_C = E_G$

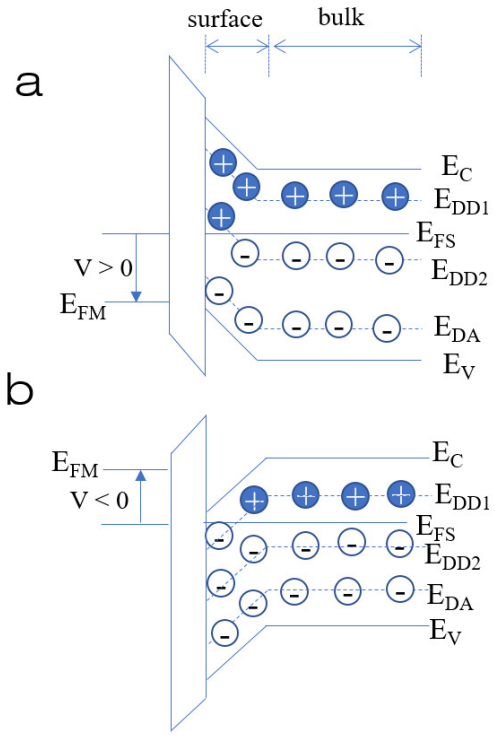

FIG. 1. Band diagram of CZT MIS device with (a) negative- and (b) positive-bias on the metal. E_{DD2} located at the middle acts as a donor in negative bias and as an acceptor in positive bias on the semiconductor's surface. If the concentration of E_{DD2} is high enough, it will result in drastic variation in capacitance with a small change in bias.

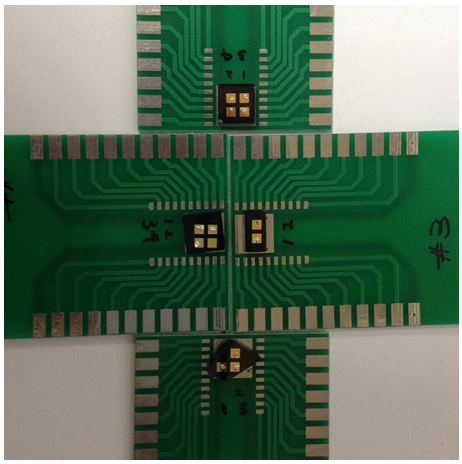

FIG. 2. Photograph of MIS CZT device mounted on a PCB board for C-V measurements. Two CZT samples are low resistivity, and two are semi-insulating.

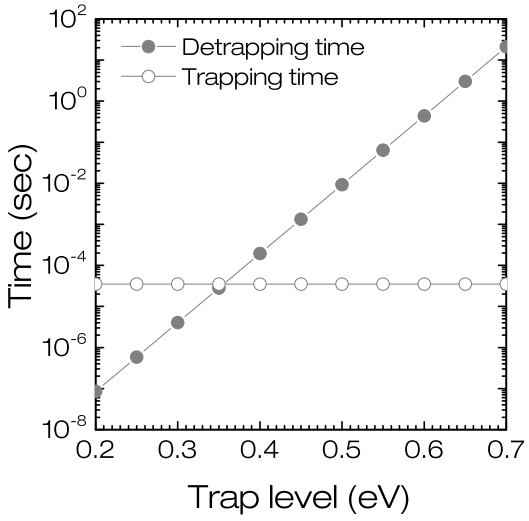

FIG. 3. The trapping and detrapping time as a function of the trap level for CZT at room temperature, assuming an average trap cross section of 10^{-13} cm^2 and the trap concentrations of 10^{12} cm^{-3}.

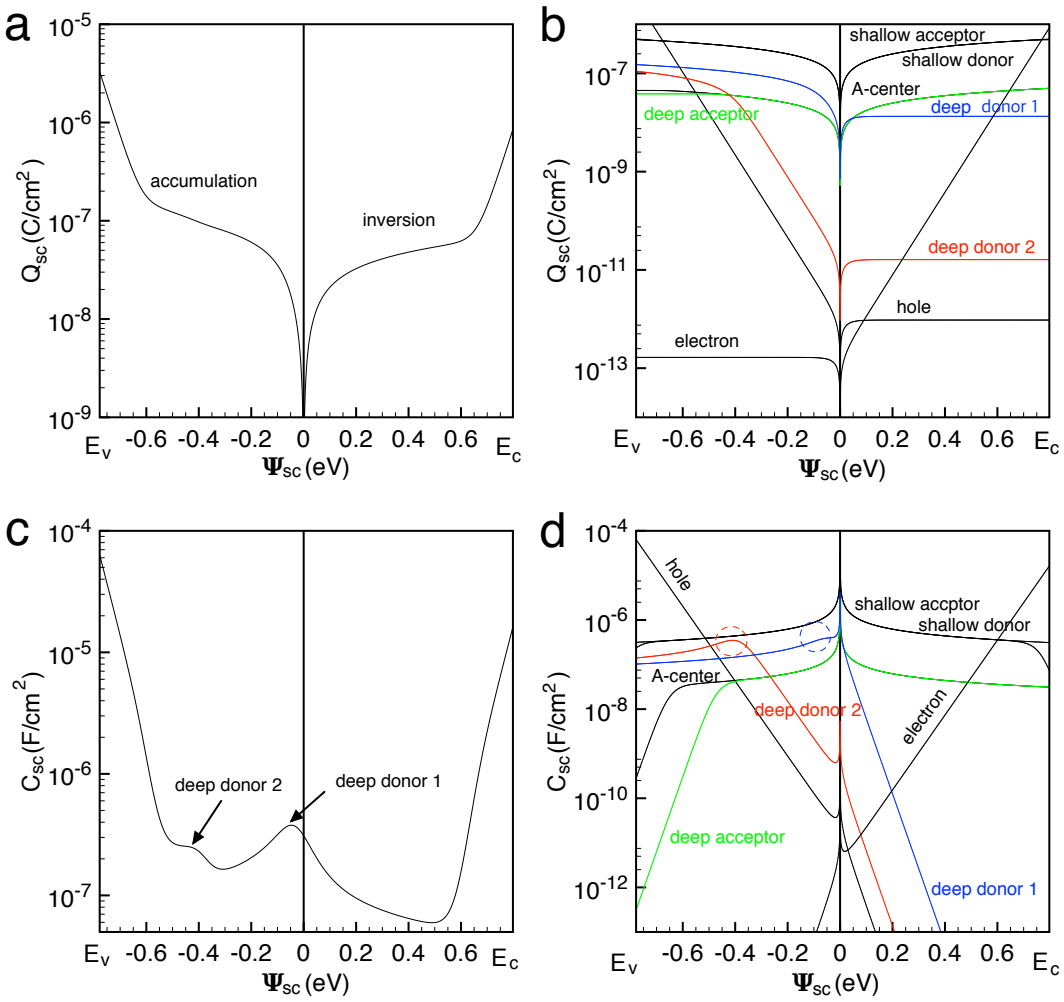

FIG. 4. Simulated (a) total charge per area in the space-charge layer (SCL), (b) charge contribution by each trap, (c) total capacitance per area in the SCL, and, (d) capacitance contribution by each trap. Trap concentrations used in the calculations are $N_{SA}=10^{16}$, $N_{AC} = 10^{14}$, $N_{DA} = 10^{14}$, $N_{DD2} = 10^{15}$, $N_{DD1} = 10^{15}$, and $N_{SD} = 10^{16}$ cm^{-3}.

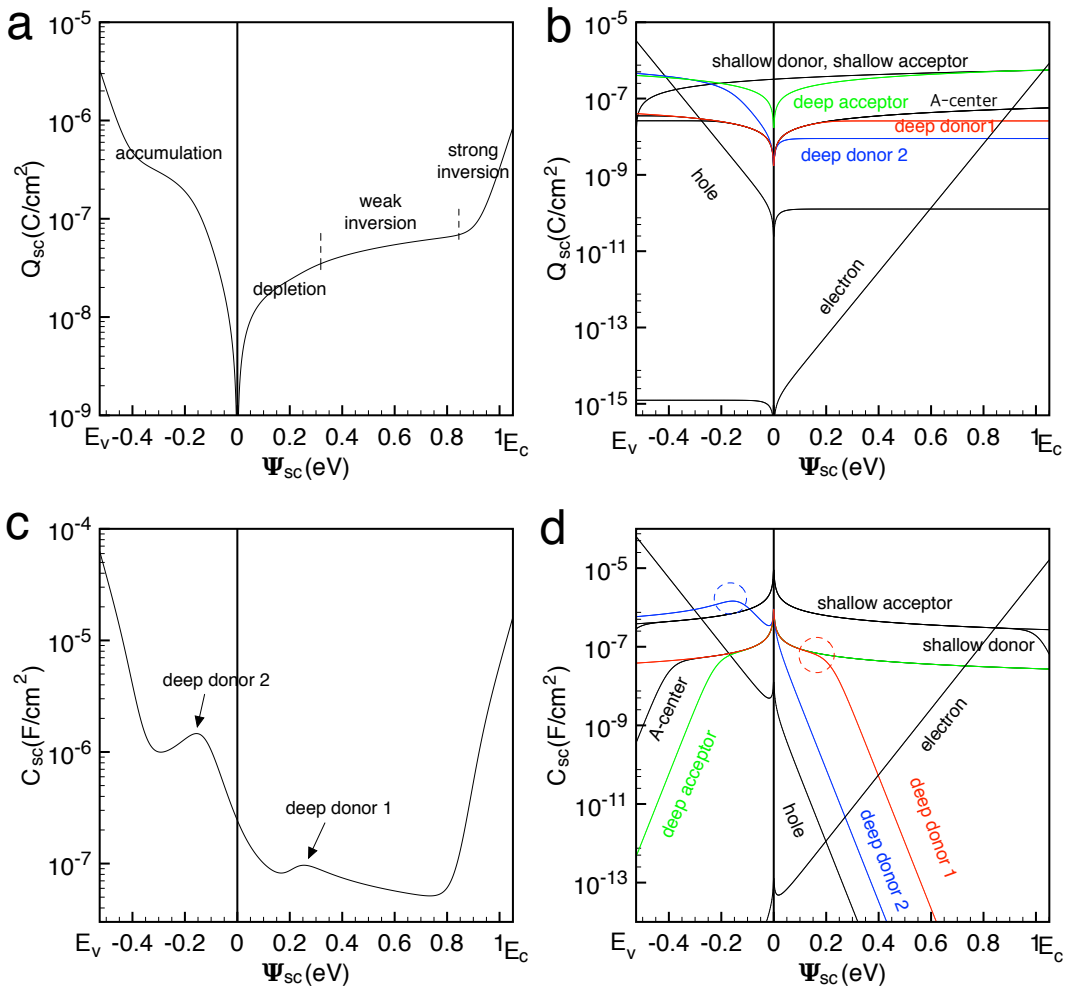

FIG. 5. (a) Simulated total charge per area in SCL, (b) charge contribution by each trap, (c) total capacitance per area in the SCL, and, (d) capacitance contribution by each trap. Trap concentrations used in the calculations are $N_{SA} = 10^{16}$, $N_{AC} = 10^{14}$, $N_{DA} = 10^{14}$, $N_{DD2} = 2.61 \times 10^{20}$, $N_{DD1} = 10^{15}$, and $N_{SD} = 10^{16}$ cm^{-3}.

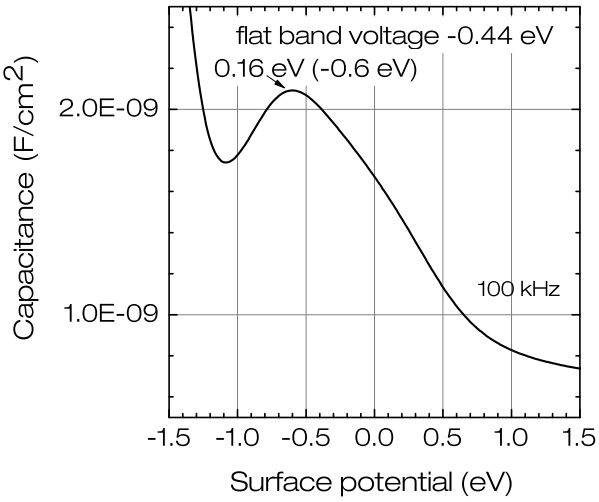

FIG. 6. Capacitance of CZT sample with 2×10^4 Ω·cm when 100-kHz frequency is applied at 300 K.

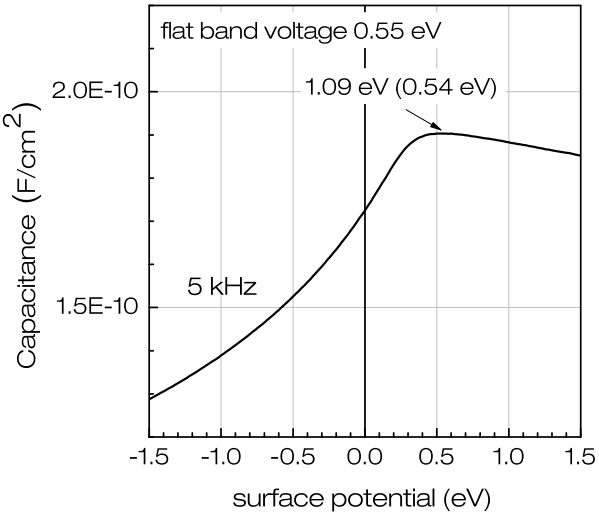

FIG. 7. Capacitance of CZT sample with 2×10^6 Ω·cm when 5-kHz frequency is applied at 300 K.